

# The Growth of Cu Nanostructures Induced by Au Nanobipyramids

Junlong Li<sup>1</sup>, Caixia Kan<sup>1,2\*</sup>, Yang Liu<sup>1</sup>, Juan Xu<sup>1</sup>, Changshun Wang<sup>1</sup>, Yuan Ni<sup>1</sup>, Shanlin Ke<sup>1</sup>

<sup>1</sup>College of Science, Nanjing University of Aeronautics and Astronautics, Nanjing 210016, P. R. China.

<sup>2</sup> Key Laboratory for Intelligent Nano Materials and Devices of the Ministry of Education, P. R. China

Email: [cxkan@nuaa.edu.cn](mailto:cxkan@nuaa.edu.cn)

**Abstract** Shapes and structures of seeds are critically important for the seed-mediated synthesis of anisotropic nanostructures. By the deposition of Cu atoms on different Au seeds, Cu nanostructures of different shapes could be synthesized. In experiments Cu nanorods formed with Au nanobipyramids as seeds, and the growth of Cu nanorods was studied through a series of experiments. It is found that the growth direction Cu nanorod is along the penta-twinned axis of Au nanobipyramids and bound by {200} side facets. For the case of low Cu<sup>2+</sup> concentration in reaction system, Cu atoms would prefer to deposit on one end of Au nanobipyramids. Nevertheless, Cu atoms would deposit on two ends of Au nanobipyramids for the case of high Cu<sup>2+</sup> concentration. Due to the different deposition and migration rates of Cu atoms at two ends of Au nanobipyramids, the Cu nanorods products exhibited different morphologies. Similarly, Cu nanopolyhedrons and Cu nanocuboids were synthesized with Au nanospheres and nanorods as seeds, respectively. Our work is of great significance for further fundamental research and applications of the Cu nanostructure-based nanomaterials in catalytic and electronic fields.

**Keywords:** Cu nanorods, Au nanobipyramids, anisotropic growth, alkyl amine

## 1. Introduction

Noble metal nanomaterials have potential applications in nanoscience and nanotechnology, because of their unique optical, electrical, thermal, catalytic properties and functionalities [1]. Over the last couple decades, noble metal (such as Au and Ag) nanostructures with various morphologies have been successfully synthesized, including nanorods, nanocubes, nanocages, nanowires and nanoprisms with well-defined shape and high purity [2-4]. Specially, due to the unique and tunable optical property originated from the localized surface plasmon resonance (LSPR), great effort has been made on the size and shape control of Au and Ag nanoparticles through chemical, physical and biological methods [5-7]. In recent years, in addition to Au and Ag, it is found that anisotropic or isotropic Cu nanostructures also exhibit tunable LSPR property in visible wavelength region [8]. Compared with Au and Ag nanostructures, Cu nanostructures exhibit high electrical conductivity, thermal conductivity, malleability and ductility [9]. And have received wide attention due to their great performance in fields related to electronics, displays, and catalysis [10-17]. Moreover, Cu is much cheaper on account of abundance in earth.

However, owing to the difficulty in reducing Cu<sup>2+</sup> or Cu<sup>+</sup> to Cu atoms in an aqueous system and the susceptibility of elemental Cu to oxidation upon exposure to air, a few reports are limited on the synthesis of Cu nanospheres, nanocubes [18-21] and nanowires [9, 22, 23]. It should be noted that Cu nanocubes covered by {200} facets have shown that higher activity and selectivity for the formation of ethylene rather than methane at low over potentials [14]. Among nanocrystals with different shapes, one dimensional structures are of particular interest for a variety of applications. For example, Cu nanowires can be used for the fabrication of touchscreens and thin-film solar cell in consequence of their high electrical conductivity and high transparency [16,24-26]. Cu nanowires and nanorods are expected to have performance in catalytic owing to the predominance of {200} facets on their side surface, as well as the presence of multiple twinned defects. While most of the reports on the synthesis of Cu nanorods are poor reproducibility [27-29]. It remains a challenge to produce Cu nanorods with high purity and adjustable aspect ratios for fundamental study about their electronic and optical properties.

In our previous work [8], we have demonstrated that single-crystal nanocubes and nanotetrahedrons could be produced in an emulsion by reducing Cu<sup>2+</sup> with glucose in the presence of hexadecylamine (HDA)

that serves as a capping agent for the Cu {200} surface. Besides, penta-twinned nanowires could also be synthesized by one-step method through changing the parameters. However, it is difficult to synthesize the Cu nanorods by this method. It is known that seed-mediated growth process is commonly applied for the formation of Au nanorods. By separating the nucleation and growth steps, seed-mediated method also offers an efficient route to the formation of Cu nanocrystals with well-controlled size, shape, and crystal structures. For example, Yin et al. demonstrated a unique strategy to induce the anisotropic growth of Cu nanorods with Au seeds containing twin plane [30]. Xia et al. reported a method for the synthesis of Pd-tipped Cu nanorods by using the poly process, taking the advantage of Pd decahedral seeds [31].

Here, we demonstrate a strategy to fabricate different Cu nanostructures by using different Au seeds, such as nanospheres, nanorods and nanobipyramids. Although these two metals are known to have a large lattice mismatch (11.4%), the formation of Cu nanorods could be achieved by the epitaxial growth on Au nanobipyramids. The diameters of the obtained Cu nanorods are about 80 nm in diameters, and the length of the Cu nanorods could be tuned by varying the growth time, as well as the concentration of Cu precursor and the amount of Au nanobipyramids in synthesis process. For the case of low concentration of CuCl<sub>2</sub>, the Au-tipped Cu nanorods could be synthesized. Moreover, the Cu atoms would deposit on the side facets of Au nanorods if using Au nanorods as seeds and Cu nanocuboids could be synthesized with Au nanorods and Cu nanopolyhedrons could be synthesized with Au nanospheres.

## 2. Experimental Section

### 2.1 Chemicals

Hexadecyltrimethylammonium chloride (CTAC, 99%), silver nitrate (AgNO<sub>3</sub>, ≥99.9%), sodium borohydride (NaBH<sub>4</sub>, ≥99.99%), hexadecyltrimethylammonium (CTAB, 99%), HCl (37%), ascorbic acid (AA, ≥99.7%), chloroauric acid (HAuCl<sub>4</sub> · 4H<sub>2</sub>O, 99.9%), trisodium citrate (C<sub>6</sub>H<sub>5</sub>Na<sub>3</sub>O<sub>7</sub> · 2H<sub>2</sub>O, ≥99%), copper(II) chloride dehydrate (CuCl<sub>2</sub>, AR, SCRC), glucose (C<sub>6</sub>H<sub>12</sub>O<sub>6</sub> · 3H<sub>2</sub>O, Reanal), hexadecylamine (HDA: C<sub>16</sub>H<sub>35</sub>N, Tech 95%), octadecylamine (ODA: C<sub>18</sub>H<sub>39</sub>N, Tech 90%), and ethanol (C<sub>2</sub>H<sub>6</sub>O, Mole Chemical, 99%) were purchased from Shanghai Chemical Reagent Co. Ltd. All reagents were used as received without further purification. Water was purified using a Milli-Q system (Millipore).

### 2.2 Synthesis of Au Nanostructure Seeds

Here, we take the synthesis of Au nanobipyramids as an example. Au nanobipyramids were obtained through a seed-mediated method. In a typical preparation procedure, the seed solution was prepared by dissolving HAuCl<sub>4</sub> (10 mL, 0.25 mM) in solution of CTAC (50 mM) and trisodium citrate (5 mM), followed by quick injection of as-prepared ice-cold NaBH<sub>4</sub> (0.25 mL, 25 mM) under stirring. Then the seed solution was thermally treated at 80 °C for 1.5 h, leading the color of seed solution gradual change from brown to red. The growth solution was obtained by adding CTAB (0.365 g), AgNO<sub>3</sub> (50 μL, 0.2 mM), HAuCl<sub>4</sub> (100 μL, 0.05 M) and HCl (400 μL, 1 M) into 9.6 mL of H<sub>2</sub>O. After adding AA (80 mL, 0.1 M) under stirring, the mixture changed from yellow to colorless. Then 80 μL seed solution was added into the growth solution and stirred for 5 min at 30 °C. Finally, the Au nanobipyramids with high purity were obtained after 2h.

Similarly, Au nanorods and nanospheres were also obtained, as reported in references [32, 33].

### 2.3 Synthesis of Cu Nanostructures

In a standard synthesis of Cu nanorods with Au nanobipyramids as seeds, 20 mL of aqueous solution with CuCl<sub>2</sub> (42 mg), ODA (200 mg) and glucose (100 mg) was strong magnetically stirred at 30 °C for 5 h to obtain light-blue emulsion. Glucose serves as a major reducing agent. Different amount of Au nanobipyramid seeds (4 mL, 8 mL and 16 mL) was added into the above mixture. After stirring for 1 h, the reaction system was transferred into an oil bath (120 °C) equipped with reflux device and heated for 3 h under magnetic stirring. The product was collected by centrifugation at 10000 RPM and washed to remove excess ODA, and finally re-dispersed in ethanol for further characterization.

Similarly, Cu nanopolyhedrons and Cu nanocuboids were also respectively obtained with Au nanospheres and nanorods as seeds.

## 2.4 Characterization

Samples for transmission electron microscopy (TEM) analysis were prepared by dropping Cu nanocrystal suspensions in distilled water onto a carbon-coated copper grid before drying at room temperature under ambient conditions. TEM analyses were carried out using a JEOL-100CX microscope operated at 100 kV. High-resolution TEM (HRTEM) images were collected on a JEOL-2011 microscope operated at 300 kV.

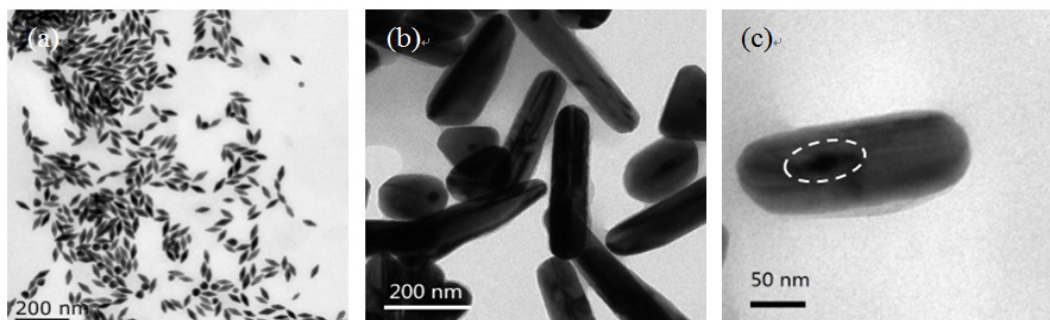


**Figure 1.** TEM images of (a) Au nanobipyramids that served as seeds for the growth of Cu nanorods; (b) Cu nanorods synthesized using the standard procedure; (c) single Cu nanorod with a clear position of Au nanobipyramid

## 3. Results and Discussion

Fig.1(a) shows a typical TEM image of Au nanobipyramids with an average length of 60 nm and width of 30 nm. The Au nanobipyramids possess the widely known penta-twinned crystal structures [34]. Fig.1(b) and (c) show TEM images of Cu nanorods synthesized using the standard procedure. The average length of Cu nanorods is about 250 nm and the diameter is about 80 nm.

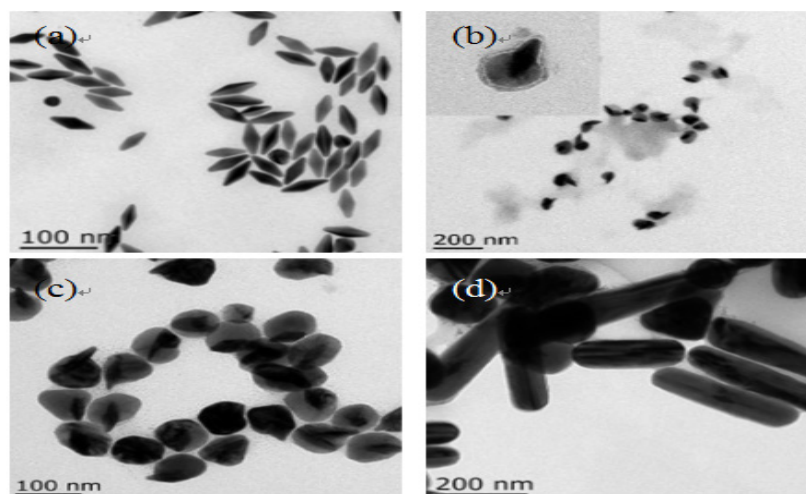


**Figure 2.** TEM images of samples of Cu nanorods obtained at different stages after adding Cu precursor (a) 0h, (b) 1h, (c) 2h and (d) 3h

To gain insight into the details of morphological evolution for the Cu nanorods, the products of different stages in the synthesis were obtained, as shown in Fig.2. For the product sampled at 1h after adding Cu precursor, it can be inferred that Cu atoms have already nucleated on the ends of Au nanobipyramids to initiate anisotropic growth shown in Fig.2(b). The symmetry breaking can be attributed to a large lattice mismatch in lattice constant between Au and Cu. With increasing time, a large amount of Cu atoms deposited on the surface of Au nanobipyramids led to growth toward the other end of Au nanobipyramids, as shown in Fig.2(c). Eventually, the rod-shaped Cu nanoparticles could be observed after reaction for 3 h, as shown in Fig.2(d).

According to the previous reports [21], ODA acting as capping agents can selectively adsorb on the Cu {200} facets, promoting the formation of Cu nanocubes and penta-twinned nanowires. And it has been shown that the existence of ODA sheath could improve the chemical stability of Cu nanorods. Because the amine group of ODA could strongly bind to the surface of Cu nanostructures, and effectively protect them from oxidation.

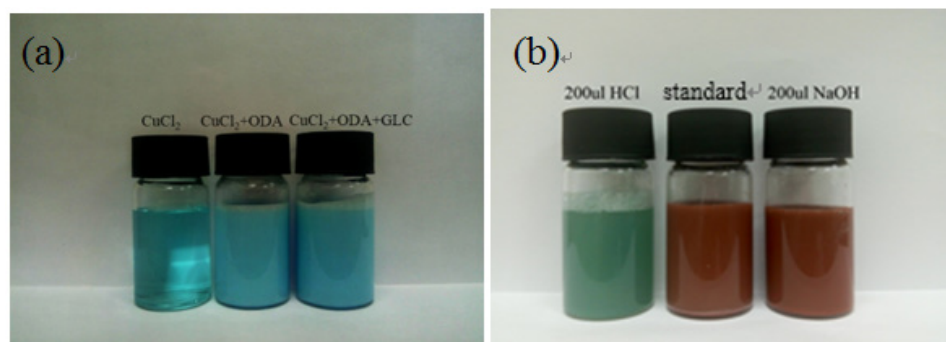


**Figure 3.** The photographs of (a)  $\text{CuCl}_2$  aqueous solution with different additives, including ODA and glucose, and (b) final products obtained by adjusting pH value with HCl (0.1 M) and NaOH (0.1 M)

In addition to its role as a capping agent combining  $\text{Cu}^{2+}$  with amine, the long-chain amine ODA could serve as a weak reducing agent in the synthesis of noble-metal nanostructures [28]. Therefore, the amount of ODA in the reaction emulsion is critical for the growth of Cu nanostructures. As can be seen from Fig.3(a), the color of solution became deep blue after addition of ODA. When the amount of ODA was reduced to 22.5 mg, the color of the emulsion had no change. The reduction could be accelerated with increasing ODA concentration. When the amount of ODA was increased to 100 mg, the color of emulsion changed from blue to red at  $t = 3$  h. Notably, the pH value also influenced the reaction process. As shown in Fig.3(b), the reaction process could normally proceed under the alkaline condition, while the process could be interrupted under the acidity condition.

As a major advantage of seed-mediated synthesis, the length of the resultant Cu nanorods could be controlled by varying the amount of Au nanobipyramids. Fig.4(a-c) show the samples of Cu nanorods obtained by adding different amount of Au nanobipyramids into reaction emulsion which contained same amount of Cu precursor. Under the condition of 16 mL of Au seeds, Cu atoms deposited on a large number of Au nanobipyramids and Cu nanorods could not be observed. With decreasing the amount of seeds, Cu nanorods formed gradually, as shown in Fig.4(b). Further decreasing the amount of seeds resulted in the formation of longer Cu nanorods, together with Cu nanocubes and Cu nanopolyhedrons (Fig.4(c)).

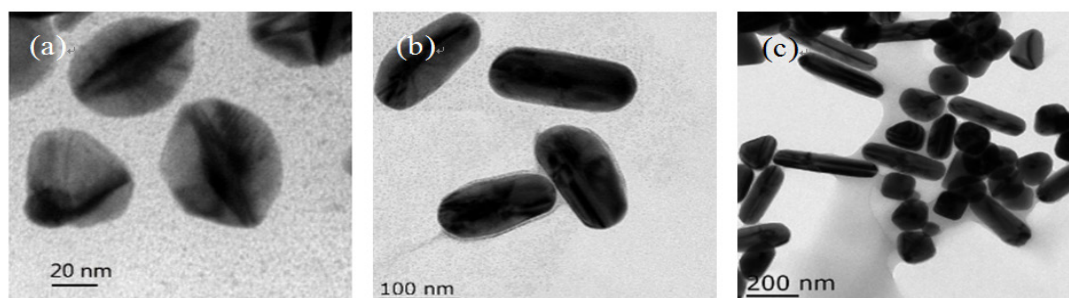


**Figure 4.** TEM images of Cu nanorods synthesized with different amount of Au nanobipyramids (a) 16 mL, (b) 8 mL and (c) 4 mL

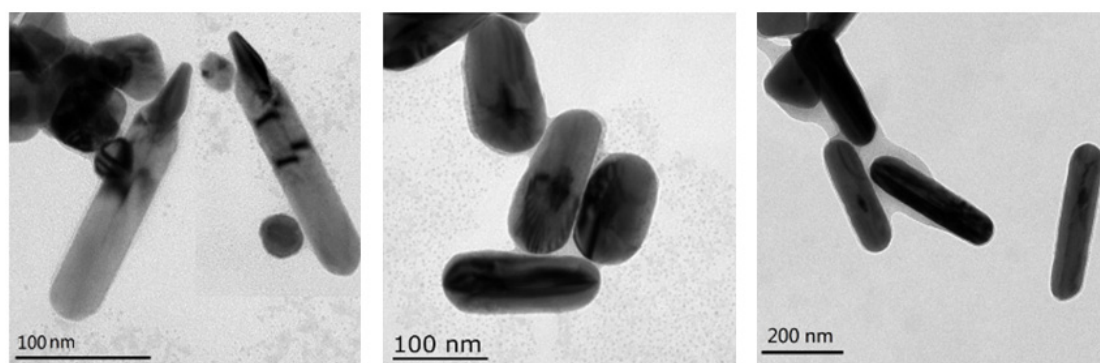


**Figure 5.** TEM images of Cu nanorods synthesized with different amount of  $\text{CuCl}_2$  (a) 12 mg, (b) 21 mg, (c) 42 mg

Interestingly, it is found that the overgrowth pattern of Cu atoms on Au seeds was influenced by the amount of  $\text{CuCl}_2$ , as indicated by Fig.5. When the amount of  $\text{CuCl}_2$  was 12 mg, the formed Cu nanorods were Au-tipped, indicating that the overgrowth was along the  $\langle 110 \rangle$  direction from one end of the Au nanobipyramids and average diameter was about 40 nm (Fig.5(a)). When the amount of  $\text{CuCl}_2$  increased up to 21 mg, the overgrowth of Cu occurred at both ends of seeds along  $\langle 110 \rangle$  direction and the diameters obviously increased (Fig.5(b)). Further increasing the amount of  $\text{CuCl}_2$  to 42 mg led to the formation of longer Cu nanorods, which revealed that the epitaxial growth of Cu occurred at both ends of Au nanobipyramids (Fig.5(c)).

To characterize the morphologies and structures of Cu nanorods, high-resolution TEM (HRTEM) was applied. Fig.6(a-c) show HRTEM images of the Au-tipped Cu nanorod obtained with less amount of  $\text{CuCl}_2$ . The lattice fringes spacing of 0.217 nm and 0.192 nm could be indexed to  $\{111\}$  and  $\{200\}$  planes of Cu crystal structure, respectively. As clearly shown in Fig.6(d), the Au nanobipyramid is located at around the center of Cu nanorod. Based on the HRTEM images (Fig.6(e-f)), it can be concluded that the Cu nanorods are bound by  $\{200\}$  side facets, together with  $\{111\}$  facets at two ends. The deposition of Cu atoms proceeded along the  $\langle 110 \rangle$  direction of Au nanobipyramids.

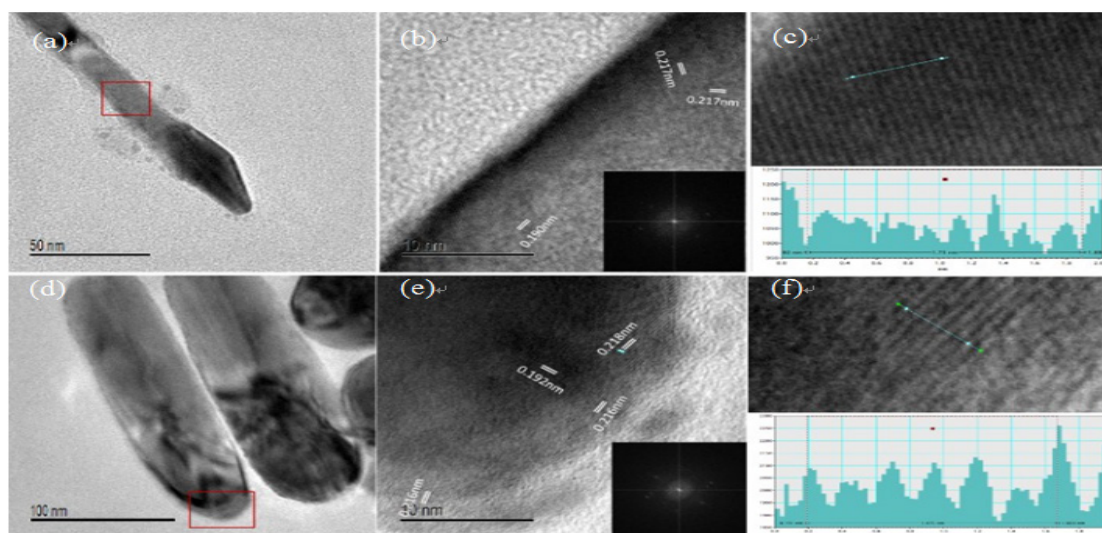


**Figure 6.** HRTEM images of Au-tipped(a) and asymmetrical (b) Cu nanorods, corresponding fast Fourier transform (FFT) patterns (b), (e) and the lattice spacing (c), (f)

Considering the influence of different facets of seeds on the anisotropic growth, we compared the Cu nanostructures by using other Au seeds with different facets, such as Au nanospheres and Au nanorods. When Au nanospheres were added into the reaction emulsion, most of the Cu nanostructures (Fig.7(a)) were irregular nanopolyhedrons, together with a few of nanorods. The nanoparticles shown in Fig.7(b) were

Cu nanocuboids synthesized with Au nanorods as seeds. Au nanorod is typically enclosed by  $\{200\}$  side facets and  $\{111\}$  end facets. A large amount of Cu atoms deposited easily on the side facets and few Cu atoms deposited on the ends of Au nanorods, resulting in the formation of Cu nanocuboids. By contrast, the products were dominated by Cu nanowires, nanotetrahedrons and nanocubes without Au seeds (Fig.7(c)).

Theoretically, we analyze the deposition process of Cu atoms on the surfaces of Au nanobipyramids using first-principles calculations. Calculations indicate that the bonding energies between Cu atoms and Au atoms of different sites on Au nanobipyramid are different ( $\Delta E = E_{\text{Au-Cu}} - E_{\text{Au}} - E_{\text{Cu}}$ ). The bonding energies on the edge and facet center of Au nanobipyramid are -0.955 eV and -1.351 eV, respectively. Therefore, the initially reduced Cu atoms will deposit on the central position of facets. Owing to the bonding energy between two Cu atoms is larger than that between Cu atom and Au atom, the subsequent reduced Cu atoms will attach around the as-deposited Cu atom.

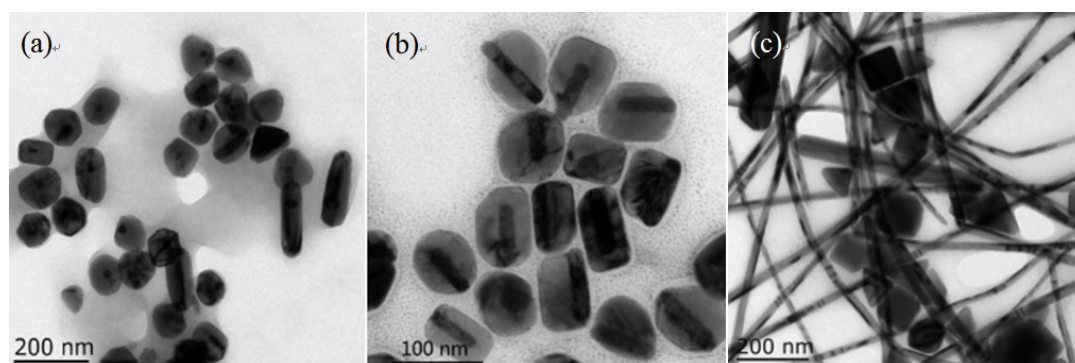


**Figure 7.** TEM images of the products synthesized with different seeds (a) Au nanospheres, (b) Au nanorods and (c) without seeds

On the basis of the above experimental results and seed-mediated growth process[35], we can propose a plausible growth mechanism, as shown in Fig.8. In our system, once Cu atoms form adatoms through heterogeneous nucleation on the surface of Au seed, those positions can serve as active sites. Subsequent attachment of Cu atoms selectively occurs on these active sites rather than other sites. The active sites distribution is mainly affected by two possible factors: (I) Collision frequency and formation of rate of Cu atoms. A fast reduction rate of  $\text{Cu}^{2+}$  produces a high concentration of Cu atoms at the nucleation stage which increases the collision frequency between the Cu atoms and the surface of Au seed. A high collision frequency promotes the nucleation of Cu atom on surface of Au seed and creates more active sites. Conversely, fewer active sites are created. (II) Cu adatoms migration from one end to the other end on the surface of Au nanobipyramid. Because of lattice mismatch and surface energy minimization, the Cu adatoms rapidly diffuse from one end to the other end of the Au nanobipyramids, altering the active site distribution and growth pattern[36-38]. In the subsequent crystal growth, the defect energy that exists along the (111) twinned planes between five crystal units limits the lateral growth as it would significantly increase the faulty area, and enhance the energy in the system. In contrast, the growth along the rod longitudinal axis causes relatively smaller increase of the faulty area and this growth is favored[39].

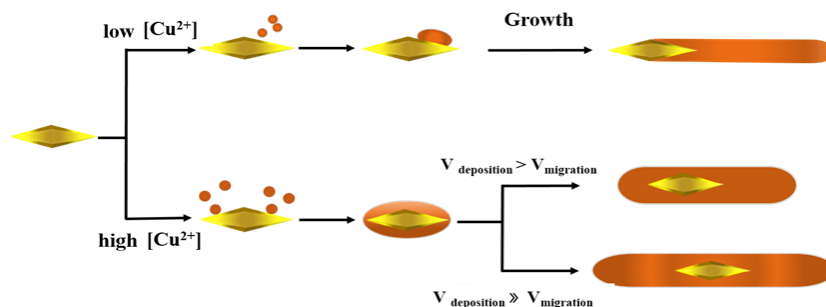


**Figure 8.** A schematic illustration for the growth of Cu nanorods with Au nanobipyramids

The seed-mediated growth mechanism for Cu nanorods is shown in Fig.8. When the reduction rate is less than the deposition rate, the newly reduced Cu atoms would deposit on the active sites around the as-deposited Cu atoms. If the deposition rate of Cu atoms is equal to the migration rate on one end of Au nanobipyramids in the initial stage, all Cu atoms can migrate to the other end, resulting in one-end growth along  $\langle 110 \rangle$  direction and the formation of Au-tipped Cu nanorods corresponding to the Fig.5(a). If the deposition rate is slightly higher than the migration rate, the Cu atoms without migration can develop to the epitaxial growth on this end. The discrepant double-ended growth pattern would cause the formation of asymmetrical Cu nanorods corresponding to the Fig.5(c). However, if the deposition rate is much higher than the migration rate, Cu atoms migration cannot produce a distinct difference between two ends resulting in the formation of symmetrical Cu nanorods. Inevitably, when the reduction rate is higher than deposition rate, Cu atoms would self-nucleate, leading to the formation of Cu nanowires, nanotetrahedrons or nanocubes, as previously reported [8]. At present our experimental results show that the highly purified production of Cu nanorods is still a challenge due to the large lattice mismatch between Au and Cu, which limits the study on the optical properties and practical applications based on the Cu nanorods. and further study is still in progress.

## 4. Conclusion

In summary, we obtained different Cu nanostructures with different Au seeds (including nanobipyramids, nanorods and nanospheres) in the presence of alkyl amine. Penta-twinned Au nanobipyramids were more suitable to induce the deposition of Cu atoms and formation of Cu nanorods, while the formations of Cu nanopolyhedrons and Cu nanocuboids could be respectively induced by Au nanospheres and nanorods. And the size of the Cu nanorods increases while increasing the amount of Cu precursor and decreasing the amount of Au nanobipyramids. We have shown the growth mechanism of Cu nanorods with different morphologies (Au-tipped, asymmetrical and symmetrical Cu nanorods). This work provides a novel and effective strategy for the rational design synthesis of anisotropic Cu nanostructures, which have potential applications in electronic and catalytic fields.

## Acknowledgements

The project was supported by the National Natural Science Foundation of China (Nos.11774171, 11374159) and Fundamental Research Funds for the Central Universities (NJ20160105). This work was also sponsored by Qing Lan Project of Jiangsu province and Graduate Innovation Base (Laboratory) Open Fund of Nanjing University of Aeronautics and Astronautics, China (kfjj20160803).

## References

1. Rao, C. N. R., Kulkarni, G. U., Thomas, P. J., Edwards, P. P., "Metal nanoparticles and their assemblies," *Chem Soc Rev* **2000**, *29* (1), 27-35.
2. Burda, C., Chen, X. B., Narayanan, R.; El-Sayed, M. A., "Chemistry and properties of nanocrystals of different shapes," *Chem Rev* **2005**, *105* (4), 1025-1102.
3. Tan, S. J., Campolongo, M. J., Luo, D.; Cheng, W. L., "Building plasmonic nanostructures with DNA," *Nat Nanotechnol*, **2011**, *6* (5), 268-276.
4. Zhao, S.Z., Duan, L.P., Xiao, C.L., Li, L., Liao, F., "Single Metal of Silver Nanoparticles in the Microemulsion for Recyclable Catalysis of 4-Nitrophenol Reduction," *Journal of Advances in Nanomaterials*, **2017**, *2* (1), 31-40.
5. Murphy, C. J., San, T. K., Gole, A. M., Orendorff, C. J., Gao, J. X., Gou, L., Hunyadi, S. E.; Li, T., "Anisotropic metal nanoparticles: Synthesis, assembly, and optical applications," *J Phys Chem B* **2005**, *109* (29), 13857-13870.
6. Perez-Juste, J., Pastoriza-Santos, I., Liz-Marzan, L. M.; Mulvaney, P., "Gold nanorods: Synthesis, characterization and applications," *Coordin Chem Rev* **2005**, *249* (17-18), 1870-1901.
7. Giljohann, D. A., Seferos, D. S., Daniel, W. L., Massich, M. D., Patel, P. C.; Mirkin, C. A., "Gold Nanoparticles for Biology and Medicine," *Angew Chem Int Edit* **2010**, *49* (19), 3280-3294.
8. Gao, Q., Kan, C. X., Li, J. L., Wei, J. J., Ni, Y.; Wang, C. S., "Alkylamine-mediated synthesis and optical properties of copper nanopolyhedrons," *Res Chem Intermediat* **2017**, *43* (5), 2753-2764.
9. Rathmell, A. R., Bergin, S. M., Hua, Y. L., Li, Z. Y.; Wiley, B. J., "The Growth Mechanism of Copper Nanowires

- and Their Properties in Flexible, Transparent Conducting Films," *Adv Mater* **2010**, *22* (32), 3558-63.
10. Vukojevic, S., Trapp, O., Grunwaldt, J. D., Kiener, C.; Schuth, F., "Quasi-homogeneous methanol synthesis over highly active copper nanoparticles," *Angew Chem Int Edit* **2005**, *44* (48), 7978-7981.
  11. Gokhale, A. A., Dumesic, J. A.; Mavrikakis, M., "On the mechanism of low-temperature water gas shift reaction on copper," *J Am Chem Soc* **2008**, *130* (4), 1402-1414.
  12. Perelaer, J., Smith, P. J., Mager, D., Soltman, D., Volkman, S. K., Subramanian, V., Korvink, J. G.; Schubert, U. S., "Printed electronics: the challenges involved in printing devices, interconnects, and contacts based on inorganic materials," *J Mater Chem* **2010**, *20* (39), 8446-8453.
  13. Roberts, F. S., Kuhl, K. P.; Nilsson, A., "High Selectivity for Ethylene from Carbon Dioxide Reduction over Copper Nanocube Electrocatalysts," *Angew Chem Int Edit* **2015**, *54* (17), 5179-5182.
  14. Xiao, B., Niu, Z. Q., Wang, Y. G., Jia, W., Shang, J., Zhang, L., Wang, D. S., Fu, Y., Zeng, J., He, W., Wu, K., Li, J., Yang, J. L., Liu, L.; Li, Y. D., "Copper Nanocrystal Plane Effect on Stereoselectivity of Catalytic Deoxygenation of Aromatic Epoxides," *J Am Chem Soc* **2015**, *137* (11), 3791-3794.
  15. Du, J. L., Chen, Z. F., Ye, S. R., Wiley, B. J.; Meyer, T. J., "Copper as a Robust and Transparent Electrocatalyst for Water Oxidation," *Angew Chem Int Edit* **2015**, *54* (7), 2073-2078.
  16. Ye, S. R., Rathmell, A. R., Chen, Z. F., Stewart, I. E.; Wiley, B. J., "Metal Nanowire Networks: The Next Generation of Transparent Conductors," *Adv Mater* **2014**, *26* (39), 6670-6687.
  17. Patra, A. K., Dutta, A.; Bhaumik, A., "Cu nanorods and nanospheres and their excellent catalytic activity in chernoselective reduction of nitrobenzenes," *Catal Commun* **2010**, *11* (7), 651-655.
  18. Ziegler, K. J., Doty, R. C., Johnston, K. P.; Korgel, B. A., "Synthesis of organic monolayer-stabilized copper nanocrystals in supercritical water," *J Am Chem Soc* **2001**, *123* (32), 7797-7803.
  19. Zhou, G. J., Lu, M. K.; Yang, Z. S., "Aqueous synthesis of copper nanocubes and bimetallic copper/palladium core-shell nanostructures," *Langmuir* **2006**, *22* (13), 5900-5903.
  20. Wang, Y. H., Chen, P. L.; Liu, M. H., "Synthesis of well-defined copper nanocubes by a one-pot solution process," *Nanotechnology* **2006**, *17* (24), 6000-6006.
  21. Jin, M. S., He, G. N., Zhang, H., Zeng, J., Xie, Z. X.; Xia, Y. N., "Shape-Controlled Synthesis of Copper Nanocrystals in an Aqueous Solution with Glucose as a Reducing Agent and Hexadecylamine as a Capping Agent," *Angew Chem Int Edit* **2011**, *50* (45), 10560-10564.
  22. Zhang, D. Q., Wang, R. R., Wen, M. C., Weng, D., Cui, X., Sun, J., Li, H. X.; Lu, Y. F., "Synthesis of Ultralong Copper Nanowires for High-Performance Transparent Electrodes," *J Am Chem Soc* **2012**, *134* (35), 14283-14286.
  23. Ye, S. R., Rathmell, A. R., Stewart, I. E., Ha, Y. C., Wilson, A. R., Chen, Z. F.; Wiley, B. J., "A rapid synthesis of high aspect ratio copper nanowires for high-performance transparent conducting films," *Chem Commun* **2014**, *50* (20), 2562-2564.
  24. Chen, J. Y., Zhou, W. X., Chen, J., Fan, Y., Zhang, Z. Q., Huang, Z. D., Feng, X. M., Mi, B. X., Ma, Y. W.; Huang, W., "Solution-processed copper nanowire flexible transparent electrodes with PEDOT:PSS as binder, protector and oxide-layer scavenger for polymer solar cells," *Nano Res* **2015**, *8* (3), 1017-1025.
  25. Stewart, I. E., Rathmell, A. R., Yan, L., Ye, S. R., Flowers, P. F., You, W.; Wiley, B. J., "Solution-processed copper-nickel nanowire anodes for organic solar cells," *Nanoscale* **2014**, *6* (11), 5980-5988.
  26. Guo, H. Z., Lin, N., Chen, Y. Z., Wang, Z. W., Xie, Q. S., Zheng, T. C., Gao, N., Li, S. P., Kang, J. Y., Cai, D. J.; Peng, D. L., "Copper Nanowires as Fully Transparent Conductive Electrodes," *Sci Rep-Uk* **2013**, *3* (7), 2323-2330.
  27. Lim, K. Y., Sow, C. H., Lin, J. Y., Cheong, F. C., Shen, Z. X., Thong, J. T. L., Chin, K. C.; Wee, A. T. S., "Laser pruning of carbon nanotubes as a route to static and movable structures," *Adv Mater* **2003**, *15* (4), 300-303.
  28. Mott, D., Galkowski, J., Wang, L. Y., Luo, J.; Zhong, C. J., "Synthesis of size-controlled and shaped copper nanoparticles," *Langmuir* **2007**, *23* (10), 5740-5745.
  29. Cha, S. I., Mo, C. B., Kim, K. T., Jeong, Y. J.; Hong, S. H., "Mechanism for controlling the shape of Cu nanocrystals prepared by the polyol process," *J Mater Res* **2006**, *21* (9), 2371-2378.
  30. Wang, Z. N., Chen, Z. Z., Zhang, H., Zhang, Z. R., Wu, H. J., Jin, M. S., Wu, C., Yang, D. R.; Yin, Y. D., "Lattice-Mismatch-Induced Twinning for Seeded Growth of Anisotropic Nano structures," *Acs Nano* **2015**, *9* (3), 3307-3313.
  31. Luo, M., Ruditskiy, A., Peng, H. C., Tao, J., Figueroa-Cosme, L., He, Z. K.; Xia, Y. N., "Penta-Twinned Copper Nanorods: Facile Synthesis via Seed-Mediated Growth and Their Tunable Plasmonic Properties," *Adv Funct Mater* **2016**, *26* (8), 1209-1216.
  32. Chen, H. J., Shao, L., Li, Q.; Wang, J. F., "Gold nanorods and their plasmonic properties," *Chem Soc Rev* **2013**, *42* (7), 2679-2724.
  33. Gao, C. B., Vuong, J., Zhang, Q., Liu, Y. D.; Yin, Y. D., "One-step seeded growth of Au nanoparticles with widely

- tunable sizes," *Nanoscale* **2012**, *4* (9), 2875-2878.
34. Sanchez-Iglesias, A., Winckelmans, N., Altantzis, T., Bals, S., Grzelczak, M.; Liz-Marzan, L. M., "High-Yield Seeded Growth of Monodisperse Pentatwinned Gold Nanoparticles through Thermally Induced Seed Twinning," *J Am Chem Soc* **2017**, *139* (1), 107-110.
35. Zhu, C., Zeng, J., Tao, J., Johnson, M. C., Schmidt-Krey, I., Blubaugh, L., Zhu, Y. M., Gu, Z. Z.; Xia, Y. N., "Kinetically Controlled Overgrowth of Ag or Au on Pd Nanocrystal Seeds: From Hybrid Dimers to Nonconcentric and Concentric Bimetallic Nanocrystals," *J Am Chem Soc* **2012**, *134* (38), 15822-15831.
36. Yang, Y., Wang, W. F., Li, X. L., Chen, W., Fan, N. N., Zou, C., Chen, X., Xu, X. J., Zhang, L. J.; Huang, S. M., "Controlled Growth of Ag/Au Bimetallic Nanorods through Kinetics Control," *Chem Mater* **2013**, *25* (1), 34-41.
37. Tsuji, M., Miyamae, N., Lim, S., Kimura, K., Zhang, X., Hikino, S.; Nishio, M., "Crystal structures and growth mechanisms of Au@Ag core-shell nanoparticles prepared by the microwave-polyol method," *Cryst Growth Des* **2006**, *6* (8), 1801-1807.
38. Tao, A. R., Habas, S.; Yang, P. D., "Shape control of colloidal metal nanocrystals". *Small* **2008**, *4* (3), 310-325.
39. Kan, C. X., Zhu, J. J.; Zhu, X. G., "Silver nanostructures with well-controlled shapes: synthesis, characterization and growth mechanisms," *J Phys D Appl Phys* **2008**, *41* (15).